DYNAMICALLY GENERATING THE QUARK-LEVEL SU(2) LINEAR SIGMA MODEL*

M.D. Scadron

Physics Department, University of Arizona
Tucson, AZ, 85721 USA

(Received August 27, 2001)

First we study Nambu-type gap equations, $\delta f_\pi = f_\pi$ and $\delta m_q = m_q$. Then we exploit the dimensional regularization lemma, subtracting quadratic from log-divergent integrals. The nonperturbative quark loop LσM solution recovers the original Gell–Mann–Levy (tree level) equations along with $m_\sigma = 2m_q$ and meson-quark coupling $g = 2\pi/\sqrt{N_{\rm c}}$. Next we use the Ben Lee null tadpole condition to reconfirm that $N_{\rm c} = 3$ even through loop order. Lastly we show that this loop order LσM (a) reproduces the (remarkably successful) Vector Meson Dominance (VMD) scheme in tree order, and (b) could be suggested as the infrared limit of low energy QCD.

PACS numbers: 12.40.Aa, 13.20.Jf, 13.20.–v

1. Introduction

To begin, we give the original [1] tree-level chiral-broken SU(2) interacting LσM Lagrangian density, but after the Spontaneous Symmetry Breaking (SSB) shift

$$\mathcal{L}^{\rm int}_{{\rm L}\sigma{\rm M}} = g\bar{\Psi}(\sigma' + i\gamma_5 \boldsymbol{\tau}\cdot\boldsymbol{\pi})\Psi + g'\sigma'(\sigma'^2 + \boldsymbol{\pi}^2) - \frac{\lambda\left(\sigma'^2 + \boldsymbol{\pi}^2\right)^2}{4}\,. \tag{1.1}$$

In Refs. [1] the couplings g, g', λ in (1.1) satisfy the quark-level Goldberger–Treiman Relation (GTR) for $f_\pi \approx 93\,$MeV and $f_\pi \sim 90\,$MeV in the Chiral Limit (CL):

$$g = \frac{m_q}{f_\pi}\,, \qquad g' = \frac{m_\sigma^2}{2f_\pi} = \lambda f_\pi\,. \tag{1.2}$$

* Presented at the XLI Cracow School of Theoretical Physics, Zakopane, Poland, June 2–11, 2001.

We work in loop order and dynamically generate mass terms in (1.1) via nonperturbative Nambu-type gap equations $\delta f_\pi = f_\pi$, $\delta m_q = m_q$. The CL $m_\pi = 0$, corresponds to $\langle 0|\partial A|\pi\rangle = 0$ for $\langle 0|A^3_\mu|\pi^0\rangle = if_\pi q_\mu$. The latter requires the GTR $m_q = f_\pi g$ to be valid in tree and loop order, fixing g, g', λ in loop order.

In Sections 2 and 3 this quark-level LσM is nonperturbatively solved via loop-order gap equations. In Sec. 4 the Nambu–Goldstone Theorem (NGT) is expressed in LσM language with charge radius $r_\pi = 1/m_q$ characterizing quark fusion for the tightly bound $q\bar{q}$ pion. In Sec. 5 the Lee null tadpole sum is shown to require $N_c = 3$ for the true vacuum. Sec. 6 discusses s-wave chiral cancellations in the LσM. Sec. 7 shows that VMD follows directly from the LσM. Finally, Sec. 8 suggests that this LσM is the infrared limit of nonperturbative QCD. We give our conclusions in Sec. 9.

2. Quark loop gap equations

First we compute $\delta f_\pi = f_\pi$ in the CL via the u and d quark loops shown in Fig. 1(a). Replacing f_π by m_q/g and taking the quark trace, giving $4m_q q_\mu$, the factors $m_q q_\mu$ cancel, requiring the CL Log-Divergent Gap Equation (LDGE) [2,3], $\bar{d}^4 p = d^4p/(2\pi)^4$ we obtain:

$$1 = -4iN_c\, g^2 \int \left(p^2 - m_q^2\right)^{-2} \bar{d}^4 p\,. \tag{2.1}$$

Anticipating $g \sim 320$ MeV/90MeV $\sim$3.6 from the CL GTR, this LDGE (2.1) suggests an UV cutoff $\Lambda \sim$750 MeV. Such a 750 MeV cutoff separates LσM elementary particle $\sigma(600) < \Lambda$ from bound states $\rho(770)$, $\omega(780)$, $a_1(1260) > \Lambda$. This is a $Z = 0$ compositeness condition [4], requiring $g = 2\pi/\sqrt{N_c}$. We later derive this from our Dynamical Symmetry Breaking (DSB) loop order LσM.

Next we study $\delta m_q = m_q$ in the CL, with zero current quark mass; m_q is the nonstrange constituent quark mass. The needed mass gap is formed via the quadratically divergent quark tadpole loop of Fig. 1(b); additional quark

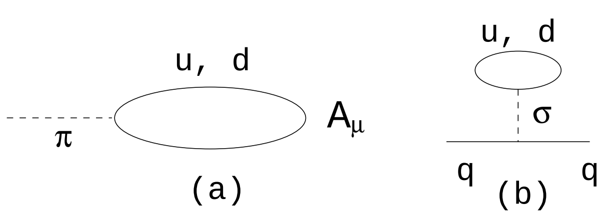

Fig. 1. Quark loop for f_π (a) and quark tadpole loop for m_q (b).

π- and σ-mediated self-energy graphs then cancel [3], giving the quadratic divergent mass gap

$$1 = \frac{8iN_{\mathrm{c}}\, g^2}{(-m_\sigma^2)} \int \left(p^2 - m_q^2\right)^{-1} \bar{\boldsymbol{d}}^4 p \,. \tag{2.2}$$

Here the $q^2 = 0$ tadpole σ propagator $(0 - m_\sigma^2)^{-1}$ means that the right-hand side of the integral in Eq. (2.2) acts as a counterterm quadratic divergent NJL [5] mass gap.

References [3] first subtract the quadratic — from the log — divergent integrals of Eqs. (2.1), (2.2) to form the dimensional regularization (dim. reg.) lemma for $2l = 4$

$$\begin{aligned} &\int \bar{\boldsymbol{d}}^4 p \left[\frac{m_q^2}{\left(p^2 - m_q^2\right)^2} - \frac{1}{p^2 - m_q^2}\right] \\ &= \lim_{l \to 2} \frac{i m_q^{2l-2}}{(4\pi)^l} \Big[\Gamma(2-l) + \Gamma(1-l)\Big] = \frac{-i m_q^2}{(4\pi)^2} \,. \end{aligned} \tag{2.3}$$

This dim. reg. lemma (2.3) follows because $\Gamma(2-l) + \Gamma(1-l) \to -1$ as $l \to 2$ due to the gamma function defining identity $\Gamma(z+1) = z\Gamma(z)$. This lemma in Eq. (2.3) is more general than dimensional regularization;

(i) use partial fractions to write

$$\frac{m^2}{(p^2 - m^2)^2} - \frac{1}{p^2 - m^2} = \frac{1}{p^2}\left[\frac{m^4}{(p^2 - m^2)^2} - 1\right], \tag{2.4}$$

(ii) integrate Eq. (2.4) via $\bar{\boldsymbol{d}}^4 p$ and neglect the latter massless tadpole $\int \bar{\boldsymbol{d}}^4 p / p^2 = 0$ (as is also done in dimensional regularization, analytic, zeta function and Pauli–Villars regularization [3]),

(iii) Wick rotate $d^4 p = i\pi^2 p_{\mathrm{E}}^2 dp_{\mathrm{E}}^2$ in the integral over Eq. (2.4) to find

$$\begin{aligned} &\int \bar{\boldsymbol{d}}^4 p \left[\frac{m^2}{(p^2 - m^2)^2} - \frac{1}{p^2 - m^2}\right] \\ &\qquad = -\frac{i m^4}{(4\pi)^2} \int_0^\infty \frac{dp_{\mathrm{E}}^2}{(p_{\mathrm{E}}^2 + m^2)^2} = \frac{-i m^2}{(4\pi)^2} \,. \end{aligned} \tag{2.5}$$

So (2.5) gives the dimensional regularization lemma (2.3); both are *regularization scheme independent.*

Following Ref. [3] we combine Eqs. (2.3) or (2.5) with the LDGE (2.1) to solve the quadratically divergent mass gap integral (2.2) as

$$m_\sigma^2 = 2m_q^2 \left(1 + \frac{g^2 N_{\rm c}}{4\pi^2}\right) . \tag{2.6}$$

Also the Fig. 2 quark bubble plus tadpole graphs dynamically generate the σ mass [3]:

$$m_\sigma^2 = 16 i N_{\rm c} g^2 \int \bar{\boldsymbol{d}}^4 p \left[\frac{m_q^2}{\left(p^2 - m_q^2\right)^2} - \frac{1}{p^2 - m_q^2} \right] = \frac{N_{\rm c} g^2 m_q^2}{\pi^2}, \tag{2.7}$$

where we have deduced the rhs of Eq. (2.7) by using (2.3) or (2.5). Finally, solving the two equations (2.6) and (2.7) for the two unknowns m_σ^2/m_q^2 and $g^2 N_{\rm c}$, one finds [3]

$$m_\sigma = 2m_q, \qquad g = \frac{2\pi}{\sqrt{N_{\rm c}}}. \tag{2.8}$$

Not surprisingly, the lhs equation in (2.8) is the famous NJL four quark result [5], earlier anticipated for the LσM in Refs. [6]. The rhs equation in (2.8) is also the consequence of the $Z = 0$ compositeness condition [4], as noted earlier.

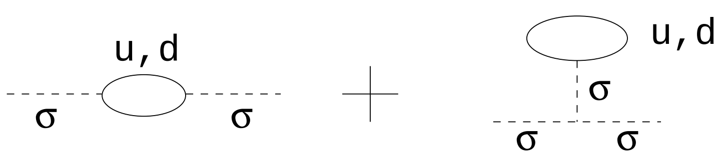

Fig. 2. Quark bubble plus quark tadpole loop for m_σ^2.

Finally, we compute m_π^2 from the analog pion bubble plus tadpole graphs of Fig. 3. Since both quark loops (ql) are quadratic divergent in the CL, one finds [2, 3]

$$\begin{aligned} m_{\pi,\,{\rm ql}}^2 &= 4 i N_{\rm c} \left[2g^2 - 4 g g' \frac{m_q}{m_\sigma^2} \right] \int \left(p^2 - m_q^2\right)^{-1} \bar{\boldsymbol{d}}^4 p = 0 \,, \\ g' &= \frac{m_\sigma^2}{2 f_\pi} \,, \end{aligned} \tag{2.9}$$

using the GTR. Not suprisingly, Eq. (2.9) is the dynamical version of the SSB (1.2).

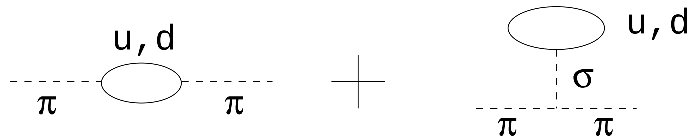

Fig. 3. Quark bubble plus quark tadpole loop for m_π^2.

3. Loop order three- and four-point functions

Having studied all two-point functions in Sec. 2, we now look at three- and four-point functions. In the CL the u and d quark loops of Fig. 4 generate $g_{\sigma\pi\pi}$ [2,3] as

$$g_{\sigma\pi\pi} = -8ig^3 N_{\rm c} m_q \int \left(p^2 - m_q^2\right)^{-2} \bar{\boldsymbol{d}}^4 p = 2gm_q \,, \tag{3.1}$$

by virtue of the LDGE (2.1). Using the GTR and $m_\sigma = 2m_q$, Eq. (3.1) reduces to

$$g_{\sigma\pi\pi} = 2gm_q = \frac{m_\sigma^2}{2f_\pi} = g' \,. \tag{3.2}$$

In effect, the $g_{\sigma\pi\pi}$ loop of Fig. 4 "shrinks" to the LσM cubic meson coupling g' in the tree-level Lagrangian Eq. (1.1), but only when $m_\sigma = 2m_q$ and $g/m_q = 1/f_\pi$.

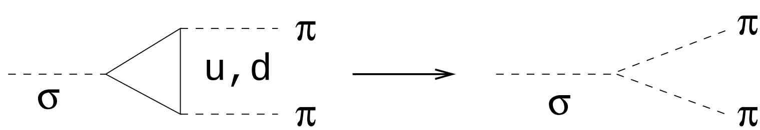

Fig. 4. Quark triangle shrinks to point for $m_\sigma \to \pi\pi$.

Next we study the four-point $\pi\pi$ quark box of Fig. 5, giving a CL log divergence [3]:

$$\lambda_{\rm box} = -8iN_{\rm c} g^4 \int \left(p^2 - m_q^2\right)^{-2} \bar{\boldsymbol{d}}^4 p = 2g^2 = \frac{g'}{f_\pi} = \lambda_{\rm tree} \,, \tag{3.3}$$

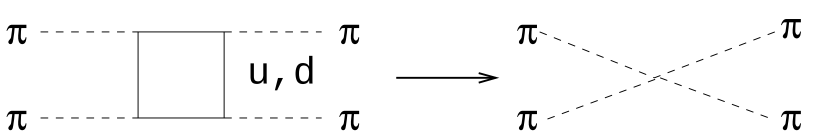

Fig. 5. Quark box shrinks to point contact for $\pi\pi \to \pi\pi$.

employing the LDGE (2.1) to reduce (3.3) to $2g^2$. Eq. (3.3) shrinks to $\lambda_{\rm tree}$, by virtue of Eq. (1.2). Substituting (2.8) into (3.3), we find $\lambda = 8\pi^2/N_{\rm c}$.

We have dynamically generated the entire LσM Lagrangian (1.1), but using the DSB true vacuum, satisfying specific values of g, g', λ in Eq. (1.1).

4. Nambu–Goldstone Theorem in LσM loop order

Having dynamically generated the chiral pion and σ as elementary, we must add to Fig. 3 the five meson loops of Fig. 6. The first bubble graph in Fig. 6 is log divergent, while the latter four quartic and tadpole graphs are quadratic divergent.

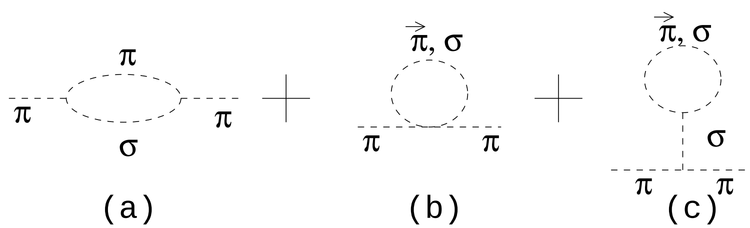

Fig. 6. Meson bubble (a), meson quartic (b), meson tadpole (c) graphs for m_π^2.

To proceed, first one uses a partial fraction identity to rewrite the log-divergent bubble graph as the difference of π and σ quadratic divergent integrals [2, 7]. Then the six meson loops (ml) of Fig. 6 can be separated into three quadratic divergent π and three quadratic divergent σ integrals [7]:

$$\begin{aligned} m^2_{\pi,\rm ml} &= (-2\lambda + 5\lambda - 3\lambda) i \int \left(p^2 - m_\pi^2\right)^{-1} \bar{\boldsymbol{d}}^4 p \\ &\quad + (2\lambda + \lambda - 3\lambda) i \int \left(p^2 - m_\sigma^2\right)^{-1} \bar{\boldsymbol{d}}^4 p\,. \end{aligned} \tag{4.1}$$

Adding Eq. (4.1) to Eq. (2.9), the total m_π^2 in the CL is in loop order

$$m_\pi^2 = m^2_{\pi,\,\rm ql} + m^2_{\pi,\pi l} + m^2_{\pi,\sigma l} = 0 + 0 + 0 = 0\,. \tag{4.2}$$

Moreover, Eq. (4.2) is chirally regularized and renormalized because the tadpole graphs of Figs. 3 and 6(c) are already counterterm masses acting as subtraction constants.

A second aspect of the chiral pion concerns the pion charge radius r_π in the CL. First one computes the pion form factor $F_{\pi,\,\mathrm{ql}}(q^2)$ due to quark loops (ql) and then differentiates it with respect to q^2 at $q^2=0$ to find $r^2_{\pi,\,\mathrm{ql}}$ as

$$\begin{aligned} r^2_{\pi,\,\mathrm{ql}} &= \left.\frac{6dF_{\pi,\,\mathrm{ql}}\left(q^2\right)}{dq^2}\right|_{q^2=0} = 8iN_\mathrm{c}g^2\int\limits_0^1 dx6x(1-x)\int\left(p^2-m_q^2\right)^{-3}\bar{\boldsymbol{d}}^4p \\ &= 8iN_\mathrm{c}\left(\frac{4\pi^2}{N_\mathrm{c}}\right)\left(\frac{-i\pi^2}{2m_q^2 16\pi^4}\right) = \frac{1}{m_q^2}\,. \end{aligned} \tag{4.3}$$

Although r_π was originally expressed as $\sqrt{N_\mathrm{c}}/2\pi f_\pi$ [7,8], we prefer the result (4.3) or $r_\pi = 1/m_q$, as it requires the tightly bound $q\bar{q}$ pion to have the two quarks *fused* in the CL. Later we will show that $N_\mathrm{c} = 3$, $m_q \approx 325$ MeV in the CL gives $r_\pi = 1/m_q \approx 0.6$ fm. The observed r_π is [9] (0.63 ± 0.01) fm. The alternative ChPT requires $r_\pi \propto L_9$, a Low Energy Constant (LEC)! However, VMD successfully predicts

$$r_\pi^{\mathrm{VMD}} = \frac{\sqrt{6}}{m_\rho} \approx 0.63\ \mathrm{fm}\,, \tag{4.4}$$

not only accurate but r_π^{VMD} and $r_\pi^{\mathrm{L}\sigma\mathrm{M}}$ in (4.3) and (4.4) are clearly related [7].

5. Lee null tadpole sum in SU(2) LσM finding $N_\mathrm{c} = 3$

To characterize the true DSB (not the false SSB) vacuum, Lee [10] requires the *sum* of loop-order tadpoles to vanish (see Fig. 7). This tadpole sum is [3]

$$\begin{aligned} \langle\sigma'\rangle = 0 \;&=\; -i8N_\mathrm{c}g\,m_q\int\left(p^2-m_q^2\right)^{-1}\bar{\boldsymbol{d}}^4p \\ &\quad + 3ig'\int\left(p^2-m_\sigma^2\right)^{-1}\bar{\boldsymbol{d}}^4p\,. \end{aligned} \tag{5.1}$$

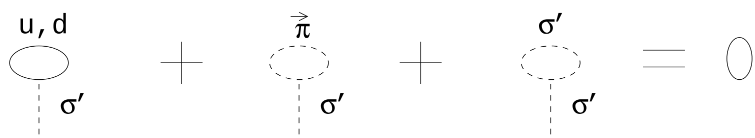

Fig. 7. Null tadpole sum for SU(2) LσM.

Replacing g by m_q/f_π, g' by $m_\sigma^2/2f_\pi$ and scaling the quadratic divergent q(or σ) loop integrals by m_q^2 (or m_σ^2), Eq. (5.1) requires [3] (neglecting the pion tadpole)

$$N_{\mathrm{c}}(2m_q)^4 = 3m_\sigma^4\,. \tag{5.2}$$

But we know from Eq. (2.8) that $2m_q = m_\sigma$, so the loop-order SU(2) LσM result (5.2) in turn *predicts* $N_{\mathrm{c}} = 3$, a satisfying result. Then the dynamically generated SU(2) loop-order LσM in Sec. 3 also predicts in the CL [3] $m_q \approx 325\,\mathrm{MeV}$, $m_\sigma \approx 650\,\mathrm{MeV}$ and $g = 2\pi/\sqrt{3} = 3.6276$, $g' = 2gm_q \approx 2.36\,\mathrm{GeV}$, $\lambda = 8\pi^2/3 \approx 26.3$.

6. Chiral s-wave cancellations in LσM

Away from the CL, the tree-order LσM requires the cubic meson coupling to be

$$g_{\sigma\pi\pi} = \frac{\left(m_\sigma^2 - m_\pi^2\right)}{2f_\pi} = \lambda f_\pi\,. \tag{6.1}$$

But at threshold $s = m_\pi^2$, so the net $\pi\pi$ amplitude then vanishes using (6.1)

$$M_{\pi\pi} = M_{\pi\pi}^{\mathrm{contact}} + M_{\pi\pi}^{\sigma\mathrm{pole}} \to \lambda + 2g_{\sigma\pi\pi}^2\left(m_\pi^2 - m_\sigma^2\right)^{-1} = 0\,. \tag{6.2}$$

In effect, the contact λ "chirally eats" the σ pole at the $\pi\pi$ threshold at tree level. Then σ poles from the cross channels predict a LσM Weinberg PCAC form [11,12]

$$\begin{aligned} M_{\pi\pi}^{abcd} &= A\delta^{ab}\delta^{cd} + B\delta^{ac}\delta^{bd} + C\delta^{ad}\delta^{bc}, \\ A^{\mathrm{L}\sigma\mathrm{M}} &= -2\lambda\left[1 - \frac{2\lambda f_\pi^2}{m_\sigma^2 - s}\right] = \left(\frac{m_\sigma^2 - m_\pi^2}{m_\sigma^2 - s}\right)\left(\frac{s - m_\pi^2}{f_\pi^2}\right). \end{aligned} \tag{6.3}$$

So the $I = 0$ s-channel amplitude $3A + B + C$ at threshold predicts a 23% enhancement of the Weinberg s-wave $I = 0$ scattering length at $s = 4m_\pi^2$, $t = u = 0$ for $m_\sigma \approx 650\,\mathrm{MeV}$ with $\varepsilon = m_\pi^2/m_\sigma^2 \approx 0.045$ and [12] (using only Eq. (6.3))

$$a_{\pi\pi}^{(0)}|_{\mathrm{L}\sigma\mathrm{M}} = \left(\frac{7+\varepsilon}{1-4\varepsilon}\right)\frac{m_\pi}{32\pi f_\pi^2} \approx (1.23)\frac{7m_\pi}{32\pi f_\pi^2} \approx 0.20 m_\pi^{-1}. \tag{6.4}$$

For $\sigma(550)$ and $\varepsilon \approx 0.063$ this LσM scattering length (6.4) increases to $0.22\,m_\pi^{-1}$. Compare this simple LσM tree order result (6.4) with the analogue ChPT $0.22\,m_\pi^{-1}$ scattering length requiring a two-loop calculation involving about 100 LECs ! These $\pi\pi$ scattering length problems should be sorted out soon by Kamiński, *et al.* [13].

In LσM loop order the analog cancellation is due to a Dirac matrix *identity* [14]

$$(\gamma\, p - m)^{-1} 2m\gamma_5(\gamma\, p - m)^{-1} = -\gamma_5(\gamma\, p - m)^{-1} - (\gamma\, p - m)^{-1}\gamma_5 \,. \quad (6.5)$$

At a soft pion momentum, Eq. (6.5) requires a σ meson to be "eaten" via a quark box-quark triangle cancellation for $a_1 \to \pi(\pi\pi)$ s wave, $\gamma\gamma \to 2\pi^0$, $\pi^- p \to \pi\pi n$ as suggested in each case by low energy data [14, 15]. Also a soft pion scalar kappa $\kappa(800\text{–}900)$ is "eaten" in $K^- p \to K^- \pi^+ n$ peripheral scattering [15].

7. VMD and the LσM

Given the implicit LDGE (2.1) UV cutoff $\Lambda \approx 750\,\text{MeV}$, the $\rho(770)$ can be taken as an external field (bound state $\bar{q}q$ vector meson). Accordingly the quark loop graphs of Fig. 8 generate the loop order $\rho\pi\pi$ coupling [2, 3]

$$g_{\rho\pi\pi} = g_\rho \left[-i4N_c g^2 \int \left(p^2 - m_q^2\right)^{-2} \bar{\boldsymbol{d}}^4 p \right] = g_\rho \,, \quad (7.1)$$

via the LDGE (2.1). While the individual udu and dud quark graphs of Fig. 8 are both linearly divergent, when added together with vertices $g_{\rho^0 uu} = -g_{\rho^0 dd}$ the net $g_{\rho\pi\pi}$ loop in Fig. 8 is log divergent. Equation (7.1) is Sakurai's VMD universality condition. Also a $\pi^+\sigma\pi^+$ meson loop added to the quark loops in Fig. 8 gives [7]

$$g_{\rho\pi\pi} = g_\rho + \frac{g_{\rho\pi\pi}}{6} \qquad \text{or} \qquad \frac{g_{\rho\pi\pi}}{g_\rho} = \frac{6}{5} \,. \quad (7.2)$$

If one first gauges the LσM Lagrangian, the inverted squared gauge coupling is related to the $q^2 = 0$ polarization amplitude as [3]

$$g_\rho^{-2} = \pi\left(0, m_q^2\right) = \frac{-8iN_c}{6} \int \left(p^2 - m_q^2\right)^{-2} \bar{\boldsymbol{d}}^4 p = \left(3g^2\right)^{-1} \,, \quad (7.3)$$

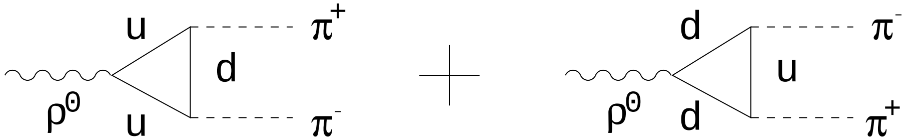

Fig. 8. Quark triangle graphs contributing to $\rho^0 \to \pi\pi$.

by virtue of the LDGE(2.1). But since we know $g = 2\pi/\sqrt{3}$, Eq. (7.3) requires $g_\rho = \sqrt{3}g = 2\pi$, reasonably near the observed values $g_{\rho\pi\pi} \approx 6.05$ and $g_\rho \approx 5.03$.

The chiral KSRF relation for the ρ mass [18] $m_\rho^2 = 2g_{\rho\pi\pi}g_\rho f_\pi^2$ coupled with this LσM implies $m_\rho^2 = 2(2\pi)^2 f_\pi^2 5/6 \approx (754\,\text{MeV})^2$, close to the observed ρ mass. Also, the dynamically generated LσM for SU(3) is given by the authors of Ref. [3].

8. LσM as infrared limit of nonperturbative QCD

We suggest five links between the LσM and the infrared limit of QCD.

(i) Quark mass: the LσM has $m_q = f_\pi\, 2\pi/\sqrt{3} \approx 325\,\text{MeV}$, while QCD has [19] $m_{\text{dyn}} = (4\pi\alpha_s/3\,\langle -\bar{\Psi}\Psi\rangle_{1\text{GeV}})^{1/3} \approx 320\,\text{MeV}$ at 1 GeV near-infrared cutoff.

(ii) Quark condensate: the LσM condensate is at infrared cutoff m_q [20]

$$\langle -\bar{\Psi}\Psi\rangle_{m_q} = i4N_{\text{c}}m_q \int \frac{\bar{\boldsymbol{d}}^4 p}{p^2 - m_q^2} = \frac{3m_q^3}{4\pi^2}\left[\frac{\Lambda^2}{m_q^2} - \ln\left(\frac{\Lambda^2}{m_q^2}+1\right)\right]$$
$$\approx (209\text{MeV})^3\,,$$

while the condensate in QCD is $\langle -\bar{\Psi}\Psi\rangle_{m_q} = 3m_{\text{dyn}}^3/\pi^2 \approx (215\,\text{MeV})^3$.

(iii) Frozen coupling strength: the LσM coupling is for $g = 2\pi/\sqrt{3}$ or $\alpha_{\text{L}\sigma\text{M}} = g^2/4\pi = \pi/3$, while in QCD $\alpha_s = \pi/4$ at infrared freezeout [21] leads to $\alpha_s^{\text{eff}} = (4/3)\alpha_s = \pi/3$.

(iv) σ mass: the LσM requires $m_\sigma = 2m_q$, while the QCD condensate gives [22] $m_{\text{dyn}} = \left(g_{\sigma qq}/m_\sigma^2\right)\langle -\bar{\Psi}\Psi\rangle_{m_\sigma}$ for $\alpha_s(m_\sigma) \approx \pi/4$, or $m_\sigma^2/m_{\text{dyn}}^2 = \pi/\alpha_s(m_\sigma^2) \approx 4$.

(v) Chiral restoration temperature T_{c}: the LσM requires [23] $T_{\text{c}} = 2f_\pi \approx 180$ MeV, while QCD computer lattice simulations find [24] $T_{\text{c}} = (173\pm 8)$ MeV.

9. Conclusions

In Secs. 2, 3 the SU(2) LσM Lagrangian was dynamically generated in all (chiral) regularization schemes, via loop gap equations, predicting the NJL σ mass $m_\sigma = 2m_q$ along with meson–quark coupling $g = 2\pi/\sqrt{N_{\text{c}}}$. Then the three-and four-point quark loops were shown to "shrink" to tree graphs, giving the meson cubic and quartic couplings $g' = m_\sigma^2/2f_\pi$, $\lambda = 8\pi^2/N_{\text{c}}$.

Next in Sec. 4 the Nambu–Goldstone Theorem was shown to hold in LσM loop order with the pion charge radius $r_\pi = 1/m_q$. In Sec. 5 the SU(2) LσM requires color number $N_c = 3$ in loop order, then predicting $m_q \approx 325$ MeV, $m_\sigma \approx 650$ MeV, $g \approx 3.63$, $\lambda \approx 26$, $r_\pi \approx 0.6$ fm in the CL.

In Sec. 6 we considered LσM chiral cancellations, both in tree and in loop order. Next, in Sec. 7 Sakurai's vector meson dominance empirically accurate scheme follows from the LσM, the latter further predicting $g_{\rho\pi\pi} = 2\pi$ and $g_{\rho\pi\pi}/g_\rho = 6/5$ along with the KSRF relation. Finally, in Sec. 8 we suggested that the LσM is the infrared limit of nonperturbative QCD.

REFERENCES

[1] M. Gell-Mann, M. Levy, *Nuovo Cimento* **16**, 705 (1960); V. de Alfaro, S. Fubini, G. Furlan, C. Rossetti, *Currents in Hadron Physics*, Ed. North Holland, 1973, Chap. 5.

[2] T. Hakioglu, M.D. Scadron, *Phys. Rev.* **D42**, 941 (1990); T. Hakioglu, M.D. Scadron, *Phys. Rev.* **D43**, 2439 (1991).

[3] R. Delbourgo, M.D. Scadron, *Mod. Phys. Lett.* **A10**, 251 (1995); R. Delbourgo, A. Rawlinson, M.D. Scadron, *Mod. Phys. Lett.* **A13**, 1893 (1998).

[4] A. Salam, *Nuovo Cimento* **25**, 224 (1962); S. Weinberg, *Phys. Rev.* **130**, 776 (1963); M.D. Scadron, *Phys. Rev.* **D57**, 5307 (1998).

[5] Y. Nambu, G. Jona-Lasinio, *Phys. Rev.* **122**, 345 (1961); also see Y. Nambu, *Phys. Rev. Lett.* **4**, 380 (1960).

[6] T. Eguchi, *Phys. Rev.* **D14**, 2755 (1976); T. Eguchi, *Phys. Rev.* **D17**, 611 (1978).

[7] A. Bramon, Riazuddin, M.D. Scadron, *J. Phys. G* **24**, 1 (1998).

[8] R. Tarrach, *Z. Phys.* **C2**, 221 (1979); S.B. Gerasimov, *Sov. J. Nucl. Phys.* **29**, 259 (1979).

[9] A.F. Grashin, M.V. Lepeshkin, *Phys. Lett.* **B146**, 11 (1984).

[10] B.W. Lee, *Chiral Dynamics*, Ed. Gordon and Breach, New York 1972, p. 12.

[11] S. Weinberg, *Phys. Rev. Lett.* **17**, 616 (1966).

[12] M.D. Scadron, *Eur. Phys. J.* **C6**, 141 (1999).

[13] R. Kamiński, *et al. Z. Phys.* **C74**, 79 (1997).

[14] A.N. Ivanov, M. Nagy, M.D. Scadron, *Phys. Lett.* **B273**, 137 (1991).

[15] L.R. Babukhadia, *et al.*, *Phys. Rev.* **D62**, 037901 (2000).

[16] S. Ishida, *et al.*, *Prog. Theor. Phys.* **95**, 745 (1996); S. Ishida, *et al.*, *Prog. Theor. Phys.* **98**, 621 (1997).

[17] See *e.g.* P. Ko, S. Rudaz, *Phys. Rev.* **D50**, 6877 (1994).

[18] K. Kawarabayashi, M. Suzuki, *Phys. Rev. Lett.* **16**, 255 (1966); Riazuddin, Fayyazudin, *Phys. Rev.* **147**, 1071 (1966).

[19] V. Elias, M.D. Scadron, *Phys. Rev.* **D30**, 647 (1984).
[20] L.R. Babukhadia, V. Elias, M.D. Scadron, *J. Phys. G* **23**, 1065 (1997).
[21] A. Mattingly, P. Stevenson, *Phys. Rev. Lett.* **69**, 1320 (1992).
[22] V. Elias, M.D. Scadron, *Phys. Rev. Lett.* **53**, 1129 (1984).
[23] N. Bilic, J. Cleymans, M.D. Scadron, *Intern. J. Mod. Phys.* **A 10**, 1160 (1995).
[24] F. Karsch, *Nucl. Phys.* **B605**, 579 (2001).